Accepted Manuscript

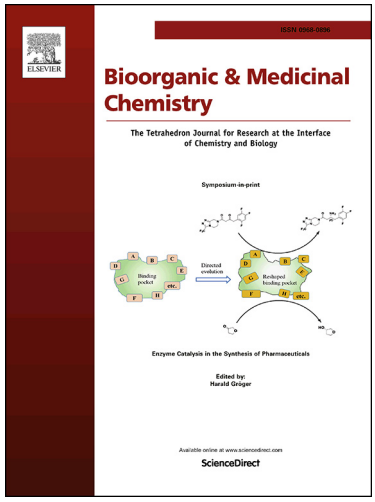

The design of 1,4-Naphthoquinone derivatives and mechanisms underlying apoptosis induction through ROS-dependent MAPK/Akt/STAT3 pathways in human lung cancer cells

Yi Zhang, Ying-Hua Luo, Xian-Ji Piao, Gui-Nan Shen, Jia-Ru Wang, Yu-Chao Feng, Jin-Qian Li, Wan-Ting Xu, Yu Zhang, Tong Zhang, Chang-Yuan Wang, Cheng-Hao Jin

PII: S0968-0896(18)31939-4
DOI: https://doi.org/10.1016/j.bmc.2019.03.002
Reference: BMC 14794

To appear in: *Bioorganic & Medicinal Chemistry*

Received Date: 15 November 2018
Revised Date: 14 February 2019
Accepted Date: 1 March 2019

Please cite this article as: Zhang, Y., Luo, Y-H., Piao, X-J., Shen, G-N., Wang, J-R., Feng, Y-C., Li, J-Q., Xu, W-T., Zhang, Y., Zhang, T., Wang, C-Y., Jin, C-H., The design of 1,4-Naphthoquinone derivatives and mechanisms underlying apoptosis induction through ROS-dependent MAPK/Akt/STAT3 pathways in human lung cancer cells, *Bioorganic & Medicinal Chemistry* (2019), doi: https://doi.org/10.1016/j.bmc.2019.03.002

This is a PDF file of an unedited manuscript that has been accepted for publication. As a service to our customers we are providing this early version of the manuscript. The manuscript will undergo copyediting, typesetting, and review of the resulting proof before it is published in its final form. Please note that during the production process errors may be discovered which could affect the content, and all legal disclaimers that apply to the journal pertain.

ACCEPTED MANUSCRIPT

The design of 1,4-Naphthoquinone derivatives and mechanisms underlying apoptosis induction through ROS-dependent MAPK/Akt/STAT3 pathways in human lung cancer cells.

Yi Zhang[a,1], Ying-Hua Luo[b,1], Xian-Ji Piao[c,1], Gui-Nan Shen[a], Jia-Ru Wang[a], Yu-Chao Feng[d], Jin-Qian Li[a], Wan-Ting Xu[a], Yu Zhang[a], Tong Zhang[a], Chang-Yuan Wang[d,*], Cheng-Hao Jin[a,d,*]

[a] Department of Biochemistry and Molecular Biology, College of Life Science & Technology, Heilongjiang Bayi Agricultural University, Daqing, Heilongjiang, 163319, China.

[b] College of Animal Science & Veterinary Medicine, Heilongjiang Bayi Agricultural University, Daqing, Heilongjiang, 163319, China.

[c] Department of Gynaecology and Obstetrics, the Fifth Affiliated Hospital of Harbin Medical University, Daqing, Heilongjiang, 163316, China.

[d] College of Food Science, Heilongjiang Bayi Agricultural University, Daqing, Heilongjiang, 163319, China.

[1] Contributed equally to this study as first authors.

[*] Corresponding authors.

E-mail addresses: jinchenghao3727@qq.com (CH. Jin), 406726021@qq.com (CY. Wang).

ACCEPTED MANUSCRIPT

ACCEPTED MANUSCRIPT

Abstract: The natural compound 1,4-naphthoquinone has potent anti-tumor activity. However, the clinical application of 1,4-naphthoquinone and its derivatives has been limited by their side effects. In this study, we attempted to reduce the toxicity of 1,4-naphthoquinone by synthesizing two derivatives: 2,3-dihydro-2,3-epoxy-2-propylsulfonyl- 5,8-dimethoxy-1,4-naphthoquinone (EPDMNQ) and 2,3-dihydro-2,3-epoxy-2- nonylsulfonyl-5,8-dimethoxy-1,4-naphthoquinone (ENDMNQ). Then we evaluated the cytotoxicity and molecular mechanisms of these compounds in lung cancer cells. EPDMNQ and ENDMNQ significantly inhibited the viabilities of three lung cancer cell lines and induced A549 cell cycle arrest at the G1 phase. In addition, they induced the apoptosis of A549 lung cancer cells by increasing the phosphorylation of p38 and c-Jun N-terminal kinase (p-JNK), and decreasing the phosphorylation of extracellular signal-related kinase (p-ERK), protein kinase B (Akt), and signal transducer and activator of transcription 3 (STAT3). Furthermore, they increased reactive oxygen species (ROS) levels in A549 cells; however, pretreatment with the ROS inhibitor N-acetyl-L-cysteine significantly inhibited EPDMNQ- and ENDMNQ-mediated apoptosis and reversed apoptotic proteins expression. In conclusion, EPDMNQ and ENDMNQ induced G1 phase cell cycle arrest and apoptosis in A549 cells via the ROS-mediated activation of mitogen activated protein kinase (MAPK), Akt and STAT3 signaling pathways.

Keywords: 1,4-naphthoquinone, Akt, apoptosis, lung cancer, MAPK, ROS, STAT3

Introduction

Lung cancer is a common malignant tumor with high morbidity and mortality. There are 230,000 new lung cancer cases worldwide each year.[1] At present, chemotherapy is the standard treatment for patients with advanced non-small cell lung cancer,[2] however, chemotherapy drugs have high toxicity and low selectivity. Therefore, the development of novel drugs with high efficacy and low toxicity is necessary.

ACCEPTED MANUSCRIPT

Apoptosis, a form of programmed cell death, is regulated by multiple signaling pathways.[3] Defects in apoptosis cause the unregulated proliferation of cancer cells, thus, inducing the apoptosis of cancer cells through multiple signaling pathways is a feasible scheme for developing novel anti-cancer agents.[4] Mitogen-activated protein kinase (MAPK) plays an important role in regulating of cell growth, differentiation, apoptosis and other important cellular physiological processes.[5] In addition, many chemotherapeutic drugs and natural compounds induce cancer cell apoptosis through the activation of the MAPK signaling pathway.[6] Therefore, this pathway may be a potential target for cancer treatment.

The Akt pathway is closely related to the development of malignant tumors, it regulates the cell cycle, apoptosis and cell proliferation.[7] Activation of Akt pathways inhibits the phosphorylation of cyclin D and E, which cannot be degraded and accumulates in cells, causing the cell to enter the S phase from G1.[8] In addition, activation of this signaling pathway also inhibits the activity of cyclin-dependent kinases (CDK) inhibitors p21 and p27, thereby promoting cell proliferation.[9,10]

Signal transducer and activator of transcription 3 (STAT3) signaling is critical for cellular processes, such as cell differentiation, growth and apoptosis, and its activation is closely related to the occurrence of various tumors, this makes STAT3 an attractive therapeutic target for cancers.[11] The persistently inhibited STAT3 down-regulates its downstream protein expression such as Bcl-2, Bcl-XL and caspase-3, which contribute to controlled proliferation of cancer cells through blocking cell cycle progression and promoting apoptosis.[12]

Reactive oxygen species (ROS) are formed during aerobic respiration of eukaryotic cells, and participate in the regulation of cell proliferation, apoptosis and other metabolic activities.[13,14] There is evidence that Increasing intracellular ROS levels can suppress the growth of cancer cells and induce cellular apoptosis by mediating MAPK and STAT3 signaling components.[15,16] Akt is representative ROS-responsive signaling pathways. When intracellular ROS continuously accumulate, Akt signaling pathway is inhibited, which eventually leads to cell cycle arrest in lung cancer cells.[17]

ACCEPTED MANUSCRIPT

The natural small compound 1,4-naphthoquinone has many biological activities, such as anti-tumor effects, and as such, has promise as a novel anti-cancer drug.[18,19] However, the application of 1,4-naphthoquinone is limited by its side effects and unclear anti-tumor mechanisms.

We previously synthesized 1,4-naphthoquinone derivatives BSNQ and OSNQ, showing good anti-tumor effects.[18] In order to further reduce the side effects of 1,4-naphthoquinone and improve its anti-tumor effects, we synthesized novel 1,4-naphthoquinone derivatives, including 2,3-dihydro-2,3-epoxy-2-propylsulfonyl-5,8-dimethoxy- 1,4-naphthoquinone (EPDMNQ) and 2,3-dihydro-2,3-epoxy-2-nonylsulfonyl-5,8- dimethoxy-1,4-naphthoquinone (ENDMNQ) after modification of its chemical structure. We elucidated the effects of EPDMNQ and ENDMNQ on the proliferation, cell cycle and ROS generation in human lung cancer A549 cells. In addition, we evaluated the molecular mechanisms underlying the apoptosis induced by these compounds.

Materials and Methods

Chemicals and reagents

The chemicals used for compound synthesis were purchased from Sigma (St. Louis, MO, USA). Solvents were of reagent grade and used without further purification. Fluorouracil (5-FU; MedChem Express, Princeton, NJ, USA) was dissolved in DMSO (Sigma) and stored at -20°C. Dulbecco's modified Eagle's medium (DMEM), fetal bovine serum (FBS), penicillin, and streptomycin were purchased from Gibco (Waltham, MA, USA). The 2´,7´-dichlorofluorescin diacetate (DCFH-DA), the Annexin V-FITC Apoptosis Detection Kit, and N-acetyl-L-cysteine (NAC) were purchased from Beyotime Biotechnology (Shanghai, China). All of the antibodies were purchased from Santa Cruz Biotechnology Inc. (Dallas, TX, USA).

Synthesis and identification of EPDMNQ and ENDMNQ

Maleic anhydride (0.12 M) and 1,4-dimethoxybenzene (0.24 M) produced 5,8-dihydroxy-1,4-naphthoquinone under the catalysis of molten aluminum chloride (142 g) and sodium chloride (28.3

ACCEPTED MANUSCRIPT

g). Then, 5,8-dihydroxy-1,4-naphthoquinone (19.0 g) reacted with sodium hyposulfite (10.6 g), dimethyl sulfate (25 mL), and sodium hydroxide (40 mL) to generate 1,4,5,8-tetramethoxynaphthalene, which produced 5,8-dimethoxy-1,4-naphthoquinone (DMNQ) under the oxidation of ceric ammonium nitrate (54.0 g). Through the catalysis of concentrated sulfuric acid (0.23 mM) and sodium dichromate (0.76 mM), DMNQ (1.38 mM) reacted with mercaptan (1.65 mM) to generate the mercaptoid compound, which was oxidized by m-chloroperoxybenzoic acid (MCPBA, 0.44 mM) to form the final products, 1,4-naphthoquinone derivatives EPDMNQ and ENDMNQ (Fig. 1A, B). EPDMNQ and ENDMNQ were validated by nuclear magnetic resonance (NMR) and mass spectrometry (MS). NMR spectra were recorded on the JNM-AL 600 (600 MHz) NMR spectrometer. Chemical shifts (d) are given in ppm downfield from tetramethylsilan as the internal standard. MS spectra were collected with the AB SCIEX API 2000 LC/MS/MS (Applied Biosystems, Inc., Foster City, CA, USA) and LCMS-IT-TOF (Shimadzu Scientific Inc., Beijing, China) systems. Finally, the two compounds were dissolved in DMSO to a stock concentration of 20 mM for subsequent experiments.

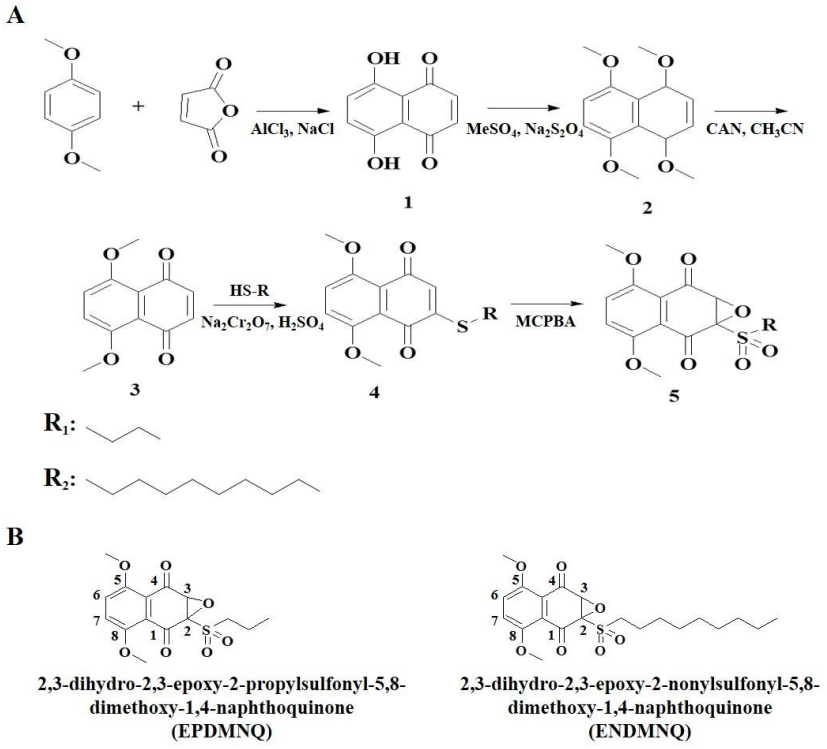

Figure 1. Synthesis of the 1,4-naphthoquinone derivatives EPDMNQ and ENDMNQ. (A) Synthetic route of EPDMNQ and ENDMNQ. (B) Structural formulas of EPDMNQ and ENDMNQ.

ACCEPTED MANUSCRIPT

Cell lines and cell cultures

The human lung cancer cell lines (A549, NCI-H23, and NCI-H460), human normal lung fibroblasts cells IMR-90, human normal liver cells QSG-7701 and human embryonic kidney cells HEK-293A were purchased from the American Type Culture Collection (Manassas, VA, USA). NCI-H23, NCI-H460 and QSG-7701 cells were cultured in RPMI 1640 medium. A549, IMR-90 and HEK-293A cells were cultured in DMEM medium. Medium contained 10% FBS, 100 U/mL penicillin, and 100 μg/mL streptomycin in a humidified 5% CO_2 incubator at 37°C.

Cell viability assay

The cell survival rate was measured by the MTT cell viability assay. A549, NCI-H23 and NCI-H460 cells in the logarithmic growth phase were seeded in 96-well plates culture at a density of 1×10^4 cells/well. Then the cells were treated with different concentrations (1, 3, 10, 30 and 100 μM) of 5-FU, EPDMNQ or ENDMNQ for 24 h. Subsequently, 20 μL MTT (5 mg/mL) was added to each well and the plate was further incubated for 2 h at 37°C. The formazan crystals were dissolved in 100 μL DMSO. The absorbance was measured at 490 nm using the Bio-Tek EXL808 microplate reader (BioTek Instruments, Winooski, VT, USA).

Cell apoptosis analysis

Cell apoptosis was detected using the Annexin V Apoptosis Detection Kit. A549 cells were cultured in 6-well plates (1×10^5 cells/well) and treated with 3 μM 5-FU, EPDMNQ or ENDMNQ for different time points (3, 6, 12 and 24 h). Following treatment, the cells were incubated with 200 μL binding buffer and stained with Annexin V-FITC and PI in the dark for 20 min, after which apoptotic cells were analyzed using fluorescence inverted microscope (Thermo Fisher Scientific Inc., Waltham, MA, USA) and flow cytometer (Beckman Coulter, Brea, CA, USA).

ACCEPTED MANUSCRIPT

Cell cycle analysis

A549 cells were cultured in 6-well plates (1×10^5 cells/well) and treated with 3 μM EPDMNQ or ENDMNQ for different time points (3, 6, 12 and 24 h). Cells were fixed in 70% ethanol at 4°C for 12 h and washed with PBS 2 times, then incubated with RNase and PI (Beyotime Biotechnology, Shanghai, China) at 37°C for 30 min. The cellular DNA content was analyzed by flow cytometry.

Western blot analysis

Equal amounts of protein (30 μg) from cell lysates were separated by 12% sodium dodecyl sulfate polyacrylamide gel electrophoresis and transferred to nitrocellulose membranes. The membranes were blocked in 5% skim milk at 37°C for 2 h, and probed with different primary antibodies against specific proteins at 4°C overnight. After washing with Tris-buffered saline and Tween 20 (TBST), the membranes were incubated with horseradish peroxidase-conjugated anti-IgG secondary antibody in TBST at room temperature for 1 h. Immunoreactive protein bands were detected with an Amersham imager (AI600; GE, Fairfield, CT, USA). The blots were analyzed using Image J 1.46r (National Institutes of Health, Bethesda, MD, USA). Apoptosis- and cell cycle-related protein levels were normalized to the matching densitometry value of β-actin as the internal control. the protein intensity of p-p38 (Thr 180 and Tyr 182), p-JNK (Thr 183 and Tyr 185), p-ERK (Tyr 204), p-Akt (Ser 473) and p-STAT3 (Tyr 705) was normalized to the expression levels of p38, JNK, ERK, Akt and STAT3, respectively.

Detection of intracellular ROS

A549 cells were pretreated with 10 mM DCFH-DA for 30 min and then incubated with 3 μM 5-FU, EPDMNQ or ENDMNQ for 3, 6, 12 and 24 h at 37°C. Next, the cells were washed twice with phosphate-buffered saline, and intracellular ROS levels were measured by flow cytometry.

ACCEPTED MANUSCRIPT

Statistical analysis

The results are expressed as the mean ± standard deviation, and all of the experiments were performed three times. The continuous data were analyzed by one-way analysis of variance followed by Tukey's post hoc tests using SPSS 19.0 statistical software, and *p<0.05, **p<0.01 and ***p<0.001 were considered to be statistically significant.

Results

Synthesis of EPDMNQ and ENDMNQ

Through a series of chemical reactions, we modified the chemical structure of 1,4-naphthoquinone and obtained two compounds, after which their hydrogen and carbon spectra were obtained by NMR. EPDMNQ: ^{1}H-NMR ($CDCl_3$, 600 MHz): δ 7.14 (s, 2H), 4.5 (s, 1H), 3.99 (s, 6H), 3.60 (m, J = 6.5 Hz, 2H), 1.9 (m, 2H), 1.1 (m, 3H); ^{13}C NMR ($CDCl_3$, 150 MHz) δ 187.2 (C-1), 184.6 (C-4), 153.4 (C-5), 152.8 (C-8), 152.7 (C-2), 130.3 (C-3), 128.3 (C-7), 120.7 (C-6), 120.3 (C-10), 120.1 (C-9), 56.8 (OCH_3), 56.4 (OCH_3), 56.9 (C-1'), 49.8 (C-2'), 14.9 (C-3'); IT-TOF/MS: m/z 364.41 (M + Na)+. ENDMNQ: ^{1}H-NMR ($CDCl_3$, 600 MHz): δ 7.14 (s, 2H), 4.5 (s, 1H), 3.99 (s, 6H), 3.60 (m, J = 6.4 Hz, 2H), 1.9 (m, 14H), 1.1 (m, 3H); ^{13}C NMR ($CDCl_3$, 150 MHz): δ191.1 (C-1), 189.3 (C-4), 154.8 (C-5), 153.4 (C-8), 152.8 (C-2), 129.9 (C-3), 128.3 (C-7), 120.7 (C-6), 120.6 (C-10), 119.1 (C-9), 56.8 (OCH_3), 56.5 (OCH_3), 56.9 (C-1'), 45.3 (C-2'), 29.7 (C-3'), 25.9 (C-4'), 20.5 (C-5'), 15.2 (C-6'), 14.7 (C-6'), 14.7 (C-7'), 14.1 (C-8') and 13.1 (C-9'); IT-TOF/MS: m/z 447.56 (M + Na)+. These results confirmed that EPDMNQ and ENDMNQ had been successfully synthesized.

EPDMNQ and ENDMNQ inhibit lung cancer cell proliferation

The MTT assay was used to determine the survival rate of three lung cancer cell lines (A549, NCI-H23, and NCI-H460). As shown in Figure 2A, EPDMNQ and ENDMNQ had significant (p<0.001) effects on cell viability, and EPDMNQ was most cytotoxic. A549 cells were more

ACCEPTED MANUSCRIPT

sensitive to the treatments (EPDMNQ/IC_{50}=2.59 μM, ENDMNQ/IC_{50}=7.54 μM) than the other cell lines, therefore these cells were used for subsequent experiments. Because the liver and kidney are the important target organ for drug toxicity testing, and human lung fibroblasts (IMR-90) are extracted from embryonic cells, their primary properties have not transformed, which can directly reflect the toxic effects in the toxicity study, so we chose the IMR-90, QSG-7701 and HEK-293A as controls. As shown in Figure 2B, compared with 5-FU, EPDMNQ and ENDMNQ had no significant cytotoxic effects on normal cells.

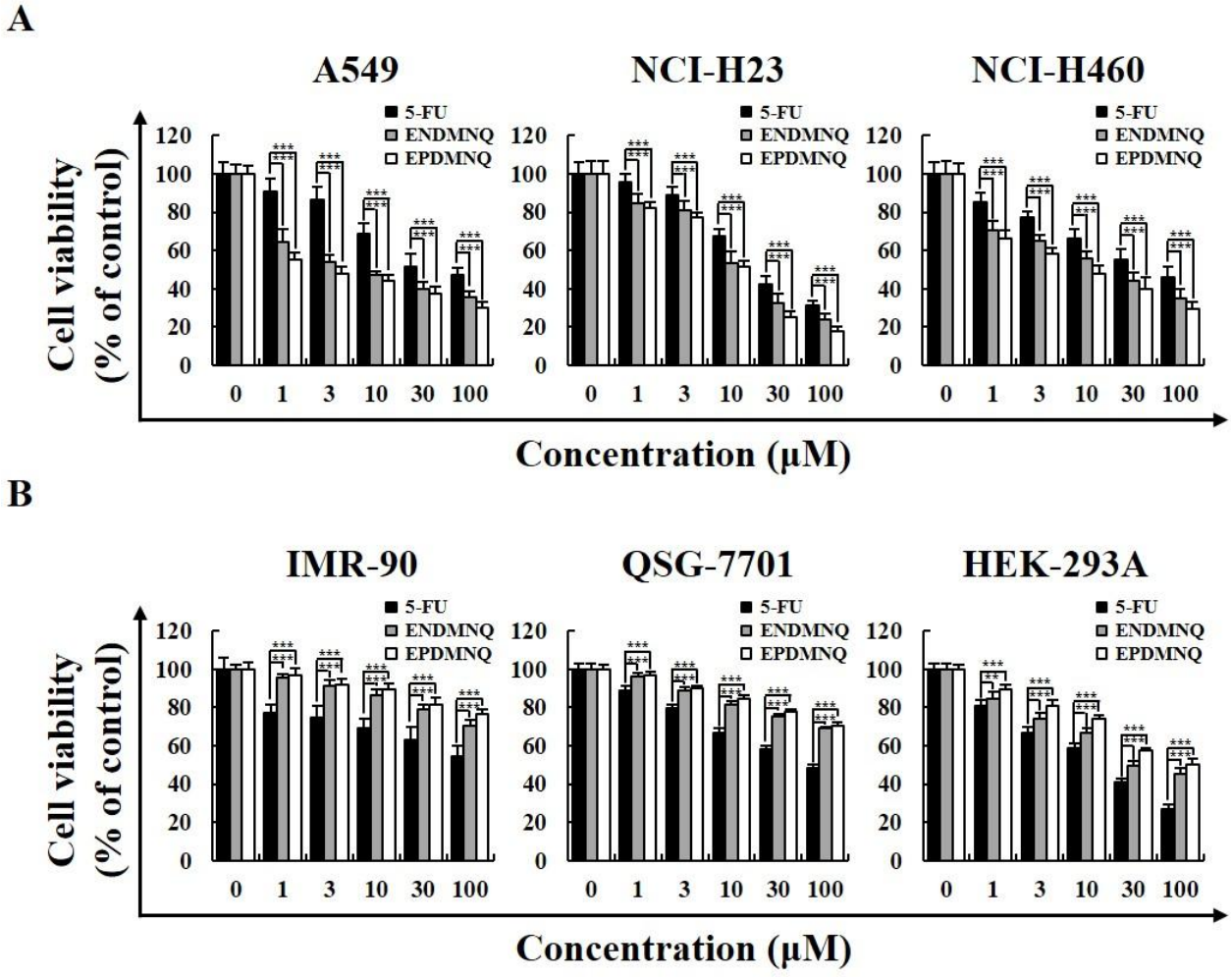

Figure 2. Cytotoxic effects of EPDMNQ and ENDMNQ on lung cancer cells. (A) Human lung cancer cell lines A549, NCI-H23, and NCI-H460 were treated with different concentrations (1, 3, 10, 30 or 100 μM) of 5-FU, EPDMNQ or ENDMNQ for 24 h. Cell viability was determined by the MTT assay. (B) Human normal lung fibroblasts cells IMR-90, human normal liver cells QSG-7701 and human embryonic kidney cells HEK-293A were treated with different concentrations (1, 3, 10,

ACCEPTED MANUSCRIPT

30 or 100 μM) of 5-FU, EPDMNQ or ENDMNQ for 24 h. Cell viability was determined by the MTT assay. The data are expressed as the means ± SD of the results from three independent experiments (* $p<0.05$, ** $p<0.01$, *** $p<0.001$ indicate significant differences).

EPDMNQ and ENDMNQ induce apoptosis in A549 cells

To verify that EPDMNQ and ENDMNQ induce apoptosis in lung cancer cells, we observed the cell morphology by Annexin V-FITC/PI staining. As shown in Figure 3A, cell shrinkage and nuclear condensation, typical apoptotic morphological features, were observed and the fluorescence intensities increased with treatment time. EPDMNQ and ENDMNQ increased A549 cell apoptosis in a time-dependent manner (Fig. 3B). To elucidate the molecular mechanisms underlying EPDMNQ- and ENDMNQ-mediated apoptosis, we used western blotting to examine the expression of apoptosis-related proteins. As shown in Figure 3C, there was a decreased expression of the anti-apoptotic protein Bcl-2, and increased expression of the pro-apoptotic protein Bad. In addition, cle-caspase-3 and cleaved poly (ADP-ribose) polymerase (cle-PARP), important biomarkers of apoptosis, were activated by EPDMNQ and ENDMNQ in a time-dependent manner.

ACCEPTED MANUSCRIPT

ACCEPTED MANUSCRIPT

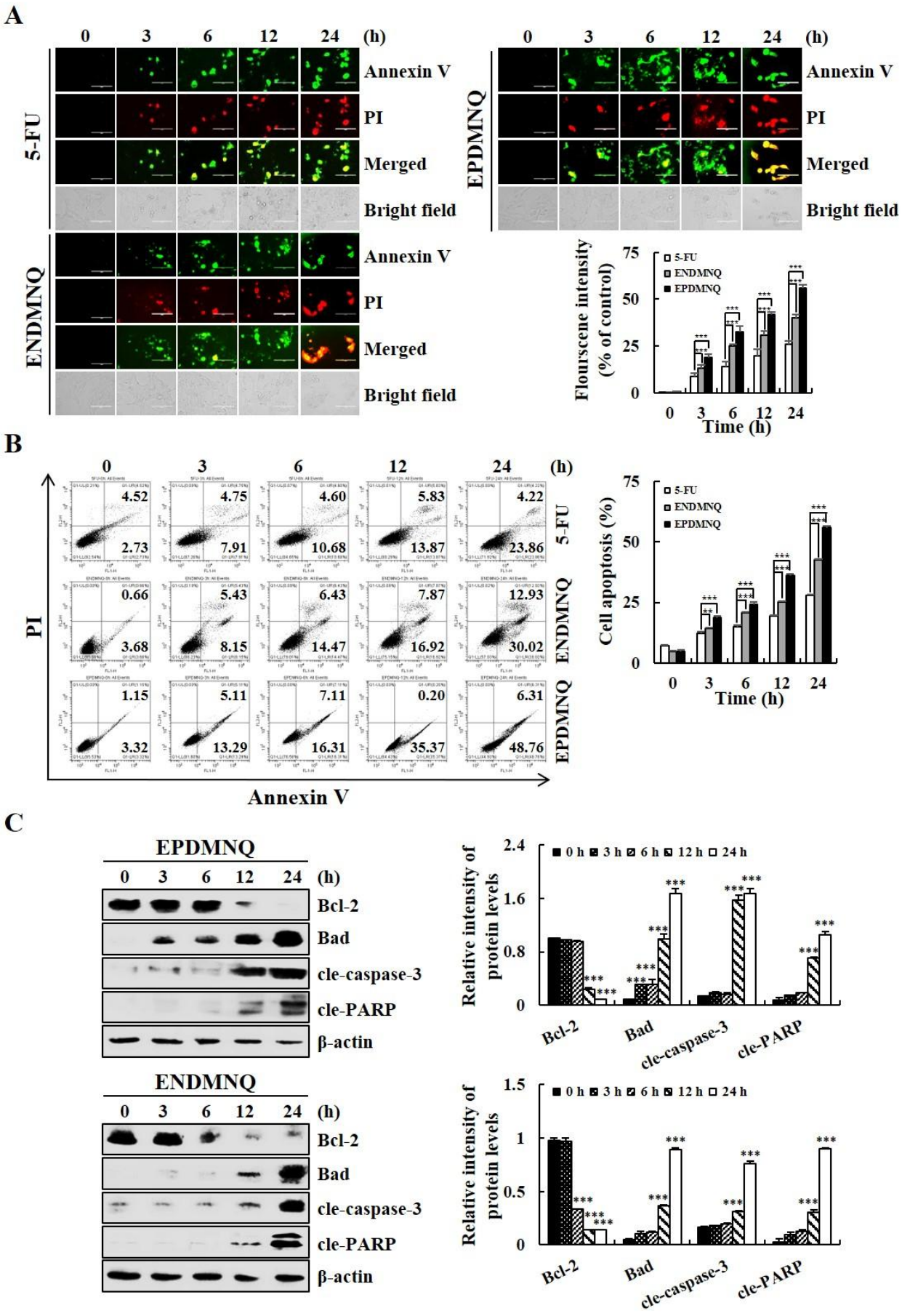

ACCEPTED MANUSCRIPT

Figure 3. EPDMNQ and ENDMNQ induce apoptosis in A549 lung cancer cells. (A) A549 cells were treated with 3 μM 5-FU, EPDMNQ or ENDMNQ for different time points (3, 6, 12 or 24 h) and stained with Annexin V-FITC/PI. (B) Apoptosis distribution was determined by flow cytometry after treatment with 3 μM 5-FU, EPDMNQ or ENDMNQ for different time points (3, 6, 12 or 24 h). (C) Apoptosis-related protein Bcl-2, Bad, cle-caspase-3, and cle-PARP was measured by western blotting. The data are expressed as the means ± SD of the results from three independent experiments (* $p<0.05$, ** $p<0.01$, *** $p<0.001$ indicate significant differences).

EPDMNQ and ENDMNQ induce cell cycle arrest at G1 phase

To investigate whether EPDMNQ and ENDMNQ-induced proliferation inhibition and apoptosis are caused by cell cycle arrest, cell cycle was analyzed with flow cytometry and the expression levels of cell cycle associated proteins were detected by western blotting. As shown in Figure 4A, after treatment with EPDMNQ or ENDMNQ, G1 phase arrest occurred in a time-dependent manner and cell numbers in S and G2 phase decreased. In addition, western blot results showed that the expression levels of CDK4/6 and cyclinD1/E were repressed, and p-Akt, p21 and p27 were increased in a time-dependent manner (Fig. 4B).

ACCEPTED MANUSCRIPT

ACCEPTED MANUSCRIPT

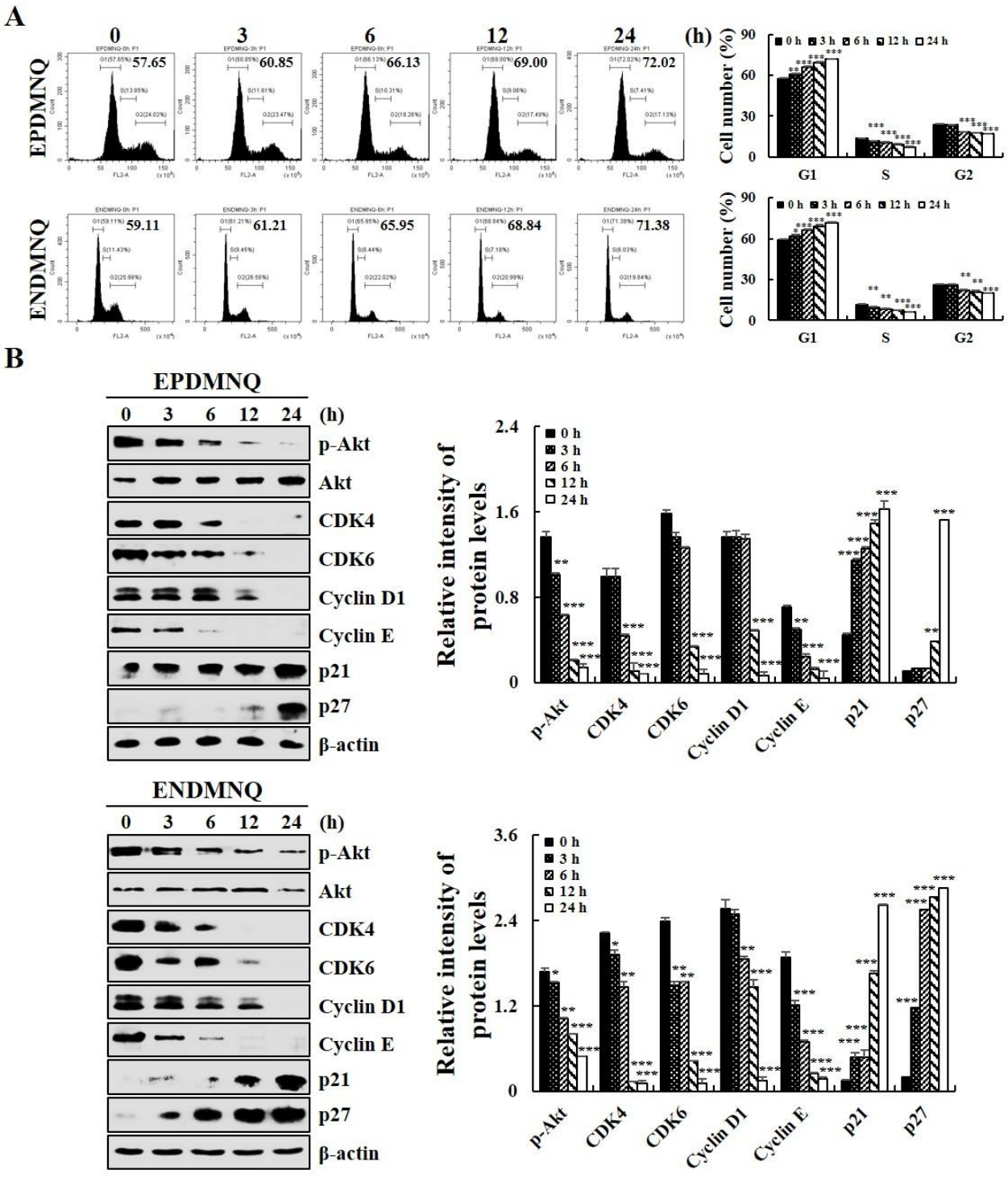

Figure 4. EPDMNQ and ENDMNQ induced G1 cycle arrest and altered the cell cycle regulatory proteins in A549 lung cancer cells. (A) Cell cycle distribution of A549 cells analysed by flow cytometer after treatment with 3 μM EPDMNQ or ENDMNQ for different time points (3, 6, 12 or 24 h). (B) The expression levels of G1 cell cycle associated proteins p-Akt, CDK4/6, cyclin D1/E, p21 and p27 were detected by western blotting after treated with 3 μM EPDMNQ or ENDMNQ for different time points (3, 6, 12 or 24 h). β-actin was used as the internal control. The data are

ACCEPTED MANUSCRIPT

expressed as the means ± SD of the results from three independent experiments (* p<0.05, ** p <0.01, *** p <0.001 indicate significant differences).

EPDMNQ and ENDMNQ regulate the MAPK and STAT3 signaling pathways

To determine the signaling pathways via which EPDMNQ and ENDMNQ mediate apoptosis, we assessed the protein expression of signaling pathways that regulate apoptosis. As shown in Figure 5A and 5B, EPDMNQ and ENDMNQ treatment significantly (p<0.001) decreased the phosphorylation of ERK and STAT3, and significantly (p<0.001) increased the phosphorylation of p38 and JNK. These results indicate that EPDMNQ and ENDMNQ induce apoptosis by activating the MAPK and STAT3 signaling pathways. SB203580 (p38 inhibitor), SP600125 (JNK inhibitor), FR180204 (ERK inhibitor) and LY10249 (Akt inhibitor) were applied to confirm the role of MAPK, Akt and STAT3 signaling pathways in the EPDMNQ or ENDMNQ -induced apoptosis and cell cycle arrest on lung cancer cells. A549 cells were pre-treated with 12.1 μM of SB203580, SP600125, FR180204 or LY10249 for 30 min followed by treatment with EPDMNQ or ENDMNQ for 24 h. The decreased protein expression levels of p-STAT3 induced by EPDMNQ or ENDMNQ were suppressed by adding the p38 inhibitor and JNK inhibitor, enhanced by adding the ERK inhibitor, but the change of cle-caspase-3 protein expression levels was completely opposite to p-STAT3 (Fig. 6A-6C). These results showed that MAPK was involved in regulating the STAT3 signaling pathway and induced apoptosis in lung cancer A549 cells. In addition, the inhibitory effect of the EPDMNQ or ENDMNQ on CDK6 and Cyclin D1 was intensified by adding the Akt inhibitor, but p27 protein expression levels were increased (Fig. 6D). These results showed that Akt signaling pathway regulates the cell cycle of lung cancer A549 cells.

ACCEPTED MANUSCRIPT

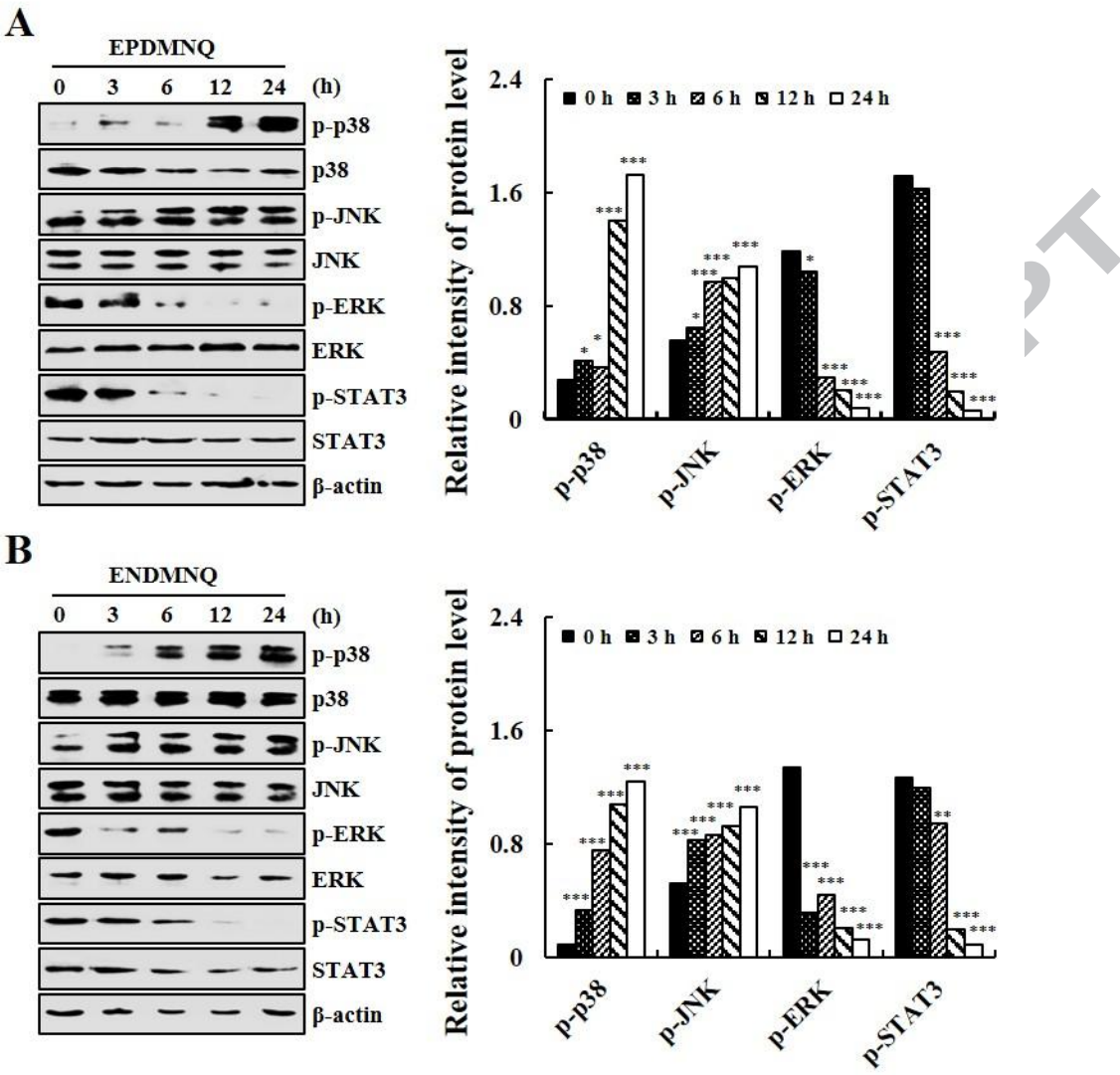

Figure 5. EPDMNQ and ENDMNQ regulate MAPK and STAT3 signaling pathway-related proteins in A549 lung cancer cells. A549 cells were treated with 3 μM EPDMNQ (A) or ENDMNQ (B) for different time points (3, 6, 12 or 24 h). The expression levels of MAPK and STAT3 pathway-related proteins were detected by western blotting. β-actin was used as the internal control. The data are expressed as the means ± SD of the results from three independent experiments (* p<0.05, ** p <0.01, *** p <0.001 indicate significant differences).

ACCEPTED MANUSCRIPT

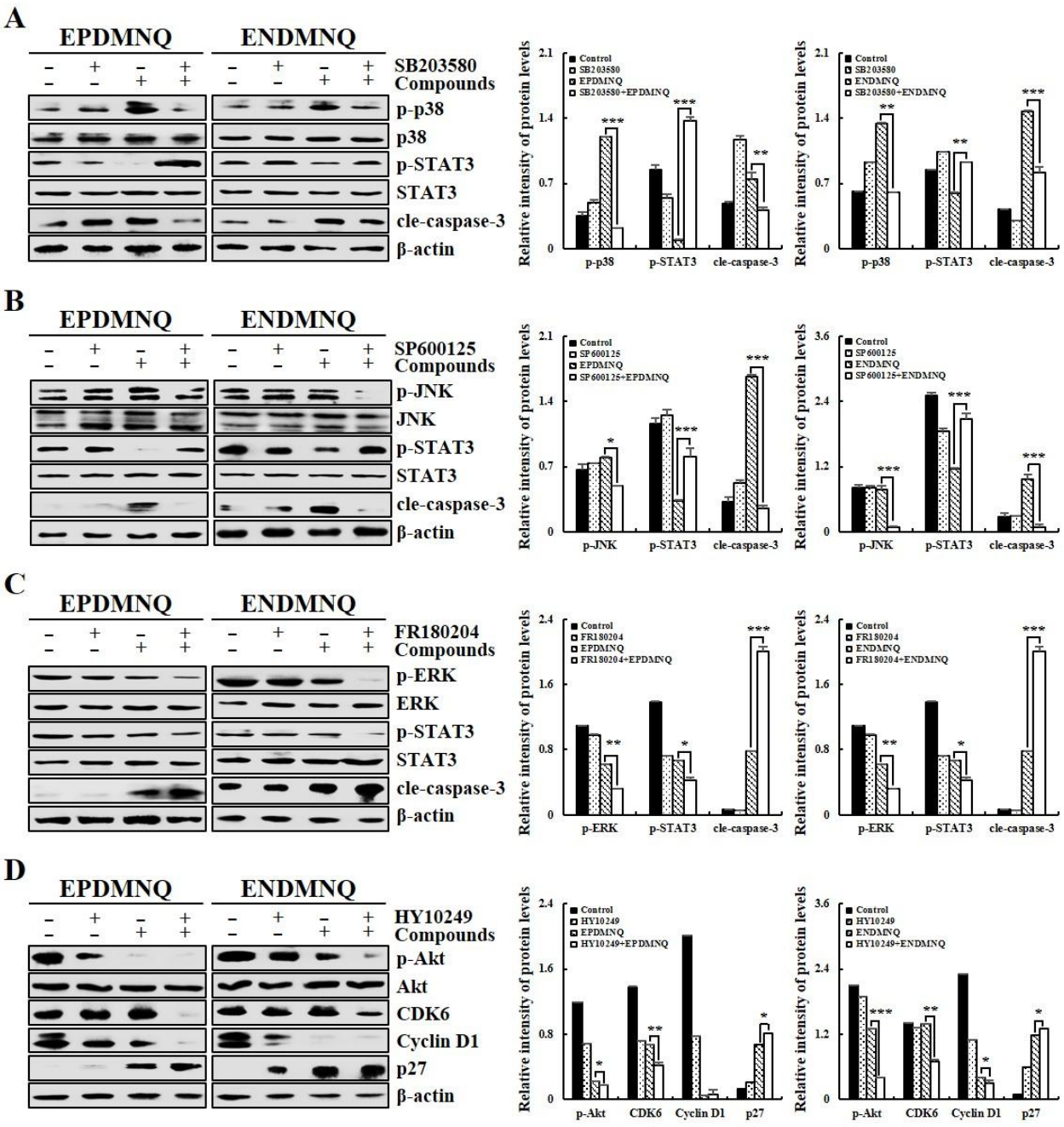

Figure 6. Effect of EPDMNQ and ENDMNQ on MAPK, Akt and STAT3 signaling pathways in A549 cells. (A) Expression of p-p38, p-STAT3, and cle-caspase-3 in the EPDMNQ or ENDMNQ and p38 inhibitor SB203580-treated A549 cells. (C) Expressions of p-JNK, p-STAT3, and cle-caspase-3 in the EPDMNQ or ENDMNQ and JNK inhibitor SP600125-treated A549 cells. (E) Expressions of p-ERK, p-STAT3, and cleaved caspase-3 in the EPDMNQ or ENDMNQ and ERK inhibitor FR180204-treated A549 cells. (E) Expressions of p-Akt, CDK6, Cyclin D1 and p27 in the EPDMNQ or ENDMNQ and Akt inhibitor HY10249-treated A549 cells. The data are expressed as

ACCEPTED MANUSCRIPT

the means ± SD of the results from three independent experiments (* p <0.05, ** p <0.01, *** p <0.001 indicate significant differences).

EPDMNQ and ENDMNQ induce ROS-mediated apoptosis in A549 cells

To investigate the correlation of ROS with EPDMNQ and ENDMNQ-mediated apoptosis in A549 cells, we used flow cytometry to detect ROS levels. EPDMNQ and ENDMNQ significantly (p<0.001) increased ROS levels in A549 cells in a time-dependent manner (Fig. 7A). However, after the addition of NAC, an ROS scavenger, apoptosis was significantly (p<0.001) suppressed (Fig. 7B). In addition, NAC reversed the effects of EPDMNQ and ENDMNQ by increasing p-ERK, p-Akt, and p-STAT3 levels and decreasing p-p38, p-JNK, cle-caspase-3, and cle-PARP levels (Fig. 7C). These data showed that EPDMNQ and ENDMNQ caused apoptosis in A549 cells by inducing ROS-mediated activation of MAPK, Akt and STAT3 signaling.

ACCEPTED MANUSCRIPT

ACCEPTED MANUSCRIPT

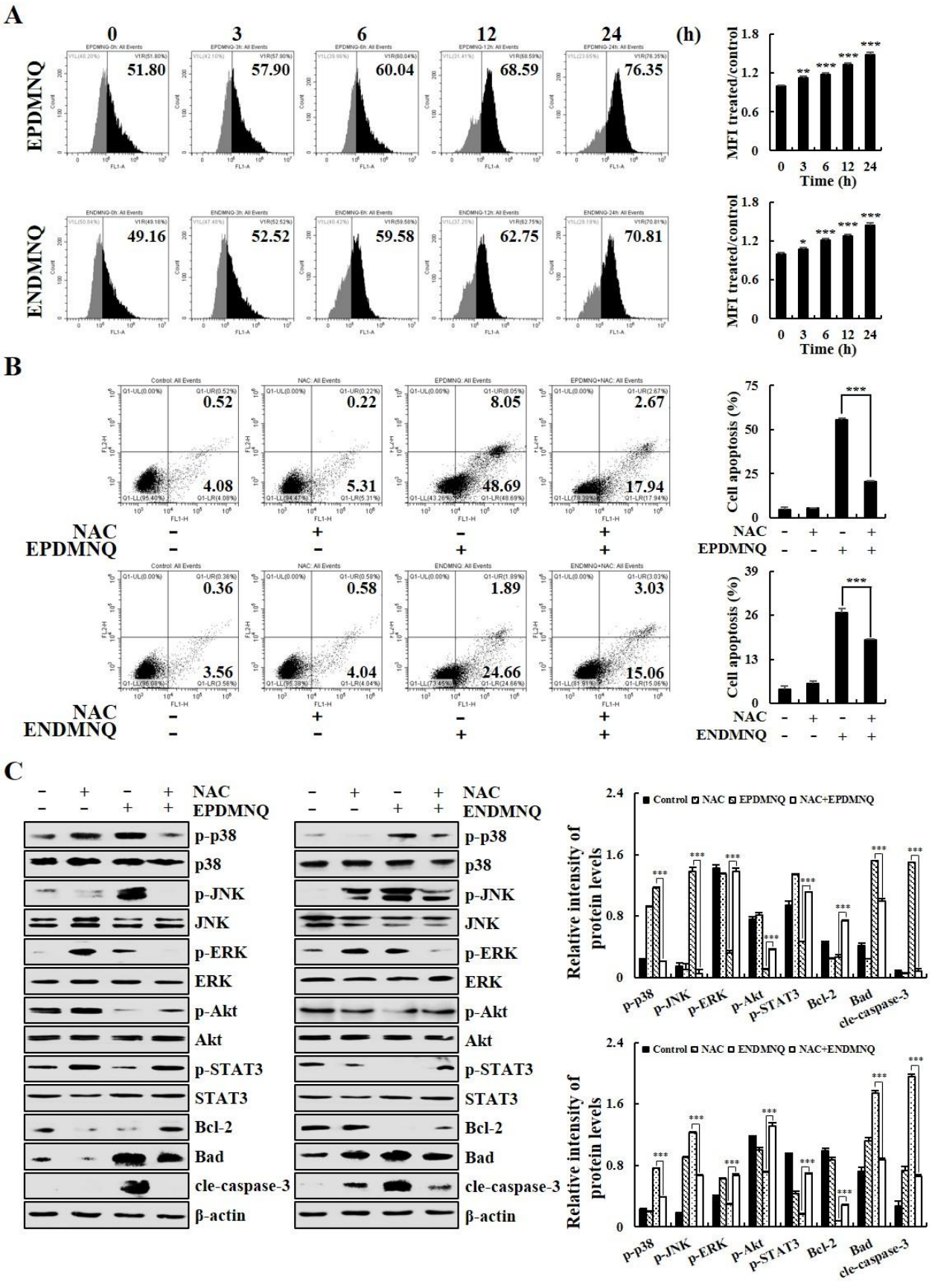

Figure 7. EPDMNQ and ENDMNQ induce ROS accumulation in A549 lung cancer cells. (A) A549 cells were treated with 3 μM 5-FU, EPDMNQ or ENDMNQ for different time points (3, 6, 12

ACCEPTED MANUSCRIPT

or 24 h) and stained with DCFH-DA (10 μM). Intracellular ROS levels were determined by flow cytometry. (B) A549 cells were treated with NAC for 30 min and then incubated with 3 μM EPDMNQ or ENDMNQ for 24 h. Cell apoptosis were determined by flow cytometry. (C) A549 cells were treated with 10 mM NAC for 30 min before treatment with EPDMNQ or ENDMNQ for 24 h. The apoptotic protein expression was measured by western blotting. The data are expressed as the means ± SD of the results from three independent experiments (* p <0.05, ** p <0.01, *** p <0.001 indicate significant differences).

Discussion

The compound 1,4-naphthoquinone is commonly found in nature, and its structure exists in a variety of drugs.[20] Research has shown that 1,4-naphthoquinone has good biological activity,[21] but its application has been limited by its potent cytotoxicity, so we used 1,4-naphthquinone as the core structure to develop novel compounds.

The structural design of 1,4-naphthquinone includes several main features. First, the bioactivity of naphthone depends on the electronegativity of the quinone ring,[22] and the strong toxicity of naphthone may be due to the hydroxyl in its structure.[23] Therefore, we introduced the methoxy group into the C5 and C8 positions to increase the electrophilicity of the quinonoid ring and reduce cytotoxicity. Second, when the branch chain of naphthquinone is introduced into sulfur atoms, the bond dissociation enthalpy significantly decreases, and the dissociation activity of the compounds significantly increases.[24] Therefore, we introduced sulfonyl at the C2 position to enhance its bioactivity. Third, by changing the length and spatial structure of the alkane chain on the C2 position, we aimed to increase the fat solubility of the compounds and study the effects of carbon chain length and volume on anti-cancer activity.[25] Based on the above principles of structural design, we ultimately synthesized EPDMNQ and ENDMNQ.

Eliminating abnormal cells through apoptosis, is an important way to maintain organism homeostasis.[26] Thus, induction of cancer cell apoptosis may be a good strategy for cancer

ACCEPTED MANUSCRIPT

treatment.[27] Mitochondria play a critical role in the regulation of apoptosis, and the mitochondrial apoptotic pathway is a common target for anti-cancer drugs.[28] Naphthquinones, such as shikonin, juglone and β-Lapachone, can induce mitochondrial apoptosis by regulating the expression of Bcl-2, Bcl-XL and Bax, resulting in activation of the caspase cascade, leading to eventual cell death.[29-31] Our experiments led to a similar conclusion, as EPDMNQ and ENDMNQ enhanced expression of the pro-apoptotic protein Bad, and inhibited the expression of Bcl-2, leading to mitochondrial-mediated apoptosis of A549 lung cancer cells.

Inhibiting the proliferation of cancer cells by regulating the cell cycle is another important strategy for cancer treatment.[32] CDK and association with regulatory cyclins regulate cell cycle by forming specialized cyclin/CDK complexes, and inhibitory proteins further regulate activity of cyclin/CDK complexes. Such as p27, p21 and p57 block the interaction of CDK4 and CDK6 with their respective targets.[33,34] Indeed, our results indicated that EPDMNQ and ENDMNQ increased the expression of p21 and p27, decreased the expression of CDK4/6 and cyclin D1/E, and eventually led to A549 cell cycle arrest at the G1 phase.

ROS are chemically reactive radicals or non-radical molecules derived from molecular oxygen.[35] ROS directly interacts with critical signaling molecules to initiate signaling in a broad variety of cellular processes, such as ROS homeostasis, target gene regulation, mitochondrial oxidative stress and apoptosis.[36-38] By inducing cells to produce a quantity of ROS, cancer cells will undergo oxidative stress, triggering mitochondrial dependent apoptosis.[39] Our results were in accordance with those studies, after EPDMNQ and ENDMNQ treatment, ROS accumulated in the cells and further activated p38 and JNK signaling pathways, inhibiting ERK and STAT3 signaling pathway, ultimately causing mitochondrial-mediated apoptosis of A549 lung cancer cells. However, after the addition of the ROS scavenger, NAC, these effects were prevented, the expression of pro-apoptotic proteins (p-p38 and p-JNK) decreased and the expression of anti-apoptotic proteins (p-ERK and p-STAT3) increased, the apoptosis induced by EPDMNQ and ENDMNQ was significantly inhibited. In addition, the results showed that the reactivation of the p38 inhibitor, JNK

ACCEPTED MANUSCRIPT

inhibitor or ERK inhibitor by EPDMNQ and ENDMNQ-inhibited the STAT3 signaling pathway, indicating that STAT3 was regulated by the MAPK signaling pathway. In other words, when the MAPK signaling pathway is activated, it can regulate the STAT3 signaling pathway and further induce apoptosis.

On the other hand, accumulating evidence has indicated that ROS serve as critical signaling molecules for cell proliferation and survival.[40] The accumulation of ROS activates the Akt, p53 and NF-κB signaling pathways, which in turn causes cell cycle arrest and eventually regulates the proliferation of cancer cells.[41,42] Our experimental results showed that ROS accumulation induced by EPDMNQ and ENDMNQ inhibited Akt signaling pathway, and further regulated the expression of CDK and cyclin, finally causing G1 phase arrest of A549 lung cancer cells. The above results showed that apoptosis regulated by MAPK and STAT3 signaling pathways and cycle arrest regulated by Akt signaling pathways were closely related to ROS generation.

The reason why EPDMNQ and ENDMNQ had low cytotoxicity in normal cells may be due to the fact that these cells have a strong antioxidant defense system and can resist oxidative stress damage. However, cancer cells have high impaired antioxidant defense mechanisms[43], which lead to ROS accumulation and oxidative stress. In addition, many studies have found that most naphthraquinones cause a metabolic imbalance in intracellular ROS levels.[44,45] Therefore, we conclude that naphthalene compounds have the same or similar targets in the process of ROS metabolism, although future studies are needed for the identification of specific targets.

In this study, we found that EPDMNQ had better anti-cancer effect than ENDMNQ, and we speculated that this difference was caused by two reasons. First, two compounds have low polarity and high lipid solubility, so EPDMNQ with a lower molecular mass is more likely to cross the cell membrane and enter the cell to perform biological functions. Second, ENDMNQ with longer carbon chain has good film-forming property, so its own effector group is not easy to be exposed and binding with the corresponding target molecule.

ACCEPTED MANUSCRIPT

In conclusion, as shown in Figure 8, our study demonstrated that EPDMNQ and ENDMNQ induced G1 phase cell cycle arrest and apoptosis in A549 cells via the ROS-mediated activation of MAPK, Akt and STAT3 signaling pathways. These results provide a basis for the development of 1,4-naphthoquinone derivatives and their application as potential anti-tumor agents for lung cancer.

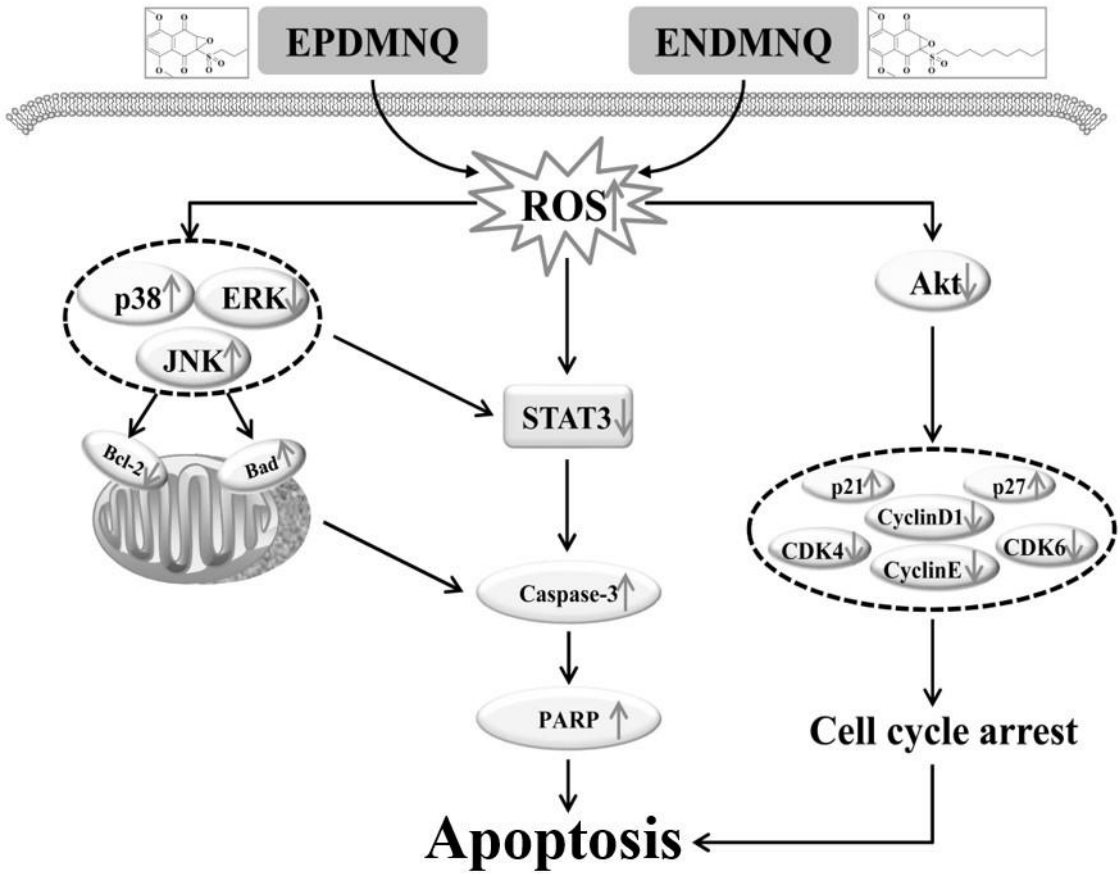

Figure 8. Overview of the pathways for EPDMNQ and ENDMNQ that induce apoptosis in A549 human lung cancer cells.

Acknowledgment

All the authors contributed to this research. YZ, YHL, XJP, and GNS took part in the analysis and data interpretation, and critical revision of the manuscript. JRW, YCF, JQL and WTX took part in evaluating the MTT assay, western blot analysis, and data interpretation. YZ and TZ conducted the fluorometric analysis. CHJ and CYW contributed to all of the experimental designs. All of the authors contributed to the critical reading and comments. This work was funded by the Multigrain

ACCEPTED MANUSCRIPT

Production and Processing Characteristic Discipline Construction Project, the Postdoctoral Scientific Research Foundation of Heilongjiang Province of China (LBH-Q13132) and National key research and development plan "Regulation and activity retention technology and application of coarse cereals active components in processing" (2017YFD0401203). In addition, we thank LetPub (www.letpub.com) for its linguistic assistance during the preparation of this manuscript.

Conflict of interest

The authors declare they have no conflict of interest.

References

1 Siegel RL, Miller KD, Jemal A. Cancer statistics, 2018. CA Cancer J Clin. 2018; 68:7-30.

2 Xu K, Liu B, Liu Y. Impact of Brachyury on epithelial-mesenchymal transitions and chemosensitivity in non-small cell lung cancer. Molecular Medicine Reports. 2015; 12:995–1001.

3 Pandurangan AK, Divya T, Kumar K, et al. Colorectal carcinogenesis: Insights into the cell death and signal transduction pathways: A review. World Journal of Gastrointestinal Oncology. 2018; 10:244–259.

4 Mehta RG, Murillo G, Naithani R, Peng X. Cancer chemoprevention by natural products: how far have we come? Pharmaceutical Research. 2010; 27:950-61.

5 Luo Z, Zhu W, Guo Q, et al. Weaning Induced Hepatic Oxidative Stress, Apoptosis, and Aminotransferases through MAPK Signaling Pathways in Piglets. Oxidative Medicine and Cellular Longevity. 2016; 2016:4768541.

6 Beccafico S, Morozzi G, Marchetti MC, et al. Artesunate induces ROS-and p38 MAPK-mediated apoptosis and counteracts tumor growth in vivo in embryonal rhabdomyosarcoma cells. Carcinogenesis. 2015; 36:1071-83.

ACCEPTED MANUSCRIPT

7 Nitulescu GM, Margina D, Juzenas P, et al. Akt inhibitors in cancer treatment: The long journey from drug discovery to clinical use (Review). Intern0ational Journal of Oncology. 2016; 48:869–885.

8 Markowska A, Pawałowska M, Lubin J, Markowska J. Signalling pathways in endometrial cancer. Contemp Oncol (Pozn). 2014;18(3):143-8.

9 Héron-Milhavet L, Franckhauser C, Rana V, et al. Only Akt1 is required for proliferation, while Akt2 promotes cell cycle exit through p21 binding. Mol Cell Biol. 2006; 26(22):8267-80.

10 Shin I, Yakes FM, Rojo F, Shin NY, Bakin AV, Baselga J, Arteaga CL. PKB/Akt mediates cell-cycle progression by phosphorylation of p27(Kip1) at threonine 157 and modulation of its cellular localization. Nat Med. 2002; 8(10):1145–52.

11 Subramaniam A, Shanmugam MK, Perumal E, et al. Potential role of signal transducer and activator of transcription (STAT)3 signaling pathway in inflammation, survival, proliferation and invasion of hepatocellular carcinoma. Biochimica et Biophysica Acta. 2013; 1835:46-60.

12 Laudisi F, Cherubini F, Monteleone G, Stolfi C. STAT3 Interactors as Potential Therapeutic Targets for Cancer Treatment. Int J Mol Sci. 2018; 19(6):1787.

13 Wang HM, Chuang SM, Su YC, et al. Downregulation of tumor-associated NADH oxidase, Tnox (ENOX2), enhances capsaicin-induced inhibition of gastric cancer cell growth. Cell Biochemistry and Biophysics. 2011; 61:355-66.

14 Di Meo S, Reed TT, Venditti P, et al. Role of ROS and RNS Sources in Physiological and Pathological Conditions. Oxidative Medicine and Cellular Longevity. 2016; 2016:1245049.

15 Guo J, Dong F, Ding L, et al. A novel drug-free strategy of nano-pulse stimulation sequence (NPSS) in oral cancer therapy: In vitro and in vivo study. Bioelectrochemistry. 2018; 123:26-33.

16 Ong JY, Yong PV, Lim YM, et al. 2-Methoxy-1,4-naphthoquinone (MNQ) induces apoptosis of A549 lung adenocarcinoma cells via oxidation-triggered JNK and p38 MAPK signaling pathways. Life Sciences. 2015; 135:158-64.

ACCEPTED MANUSCRIPT

17 Xu H, Li, X, Ding W, et al. Deguelin induces the apoptosis of lung cancer cells through regulating a ROS driven Akt pathway. Cancer Cell International. 2015; 15:25.

18 Liu C, Shen GN, Luo YH, et al. Novel 1,4-naphthoquinone derivatives induce apoptosis via ROS-mediated p38/MAPK, Akt and STAT3 signaling in human hepatoma Hep3B cells. The International Journal of Biochemistry & Cell Biology. 2018; 96:9-19.

19 Lee EB, Cheon MG, Cui J, et al. The quinone-based derivative, HMNQ induces apoptotic and autophagic cell death by modulating reactive oxygen species in cancer cells. Oncotarget. 2017; 8:99637–99648.

20 Zhang RX, Zhang T, Chen K, et al. Sample Extraction and Simultaneous Chromatographic Quantitation of Doxorubicin and Mitomycin C Following Drug Combination Delivery in Nanoparticles to Tumor-bearing Mice. Journal of Visualized Experiments: JoVE. 2017; 128.

21 Im YS, Chung Y, Won DY, et al. Apoptotic effect of Naphthoquinone derivatives on HCT116 colon cancer cells. Genes & Genomics. 2010; 32:592–598.

22 Tu T, Giblin D, Gross ML. A Structural Determinant of Chemical Reactivity and Potential Health Effects of Quinones from Natural Products. Chemical Research in Toxicology. 2011; 24:1527–1539.

23 Ollinger K, Brunmark A. Effect of hydroxy substituent position on 1,4-naphthoquinone toxicity to rat hepatocytes. The Journal of Biological Chemistry. 1991; 266:21496-503.

24 Abiko Y, Shinkai Y, Unoki T, et al. Polysulfide Na_2S_4 regulates the activation of PTEN/Akt/CREB signaling and cytotoxicity mediated by 1,4-naphthoquinone through formation of sulfur adducts. Scientific Reports. 2017; 7:4814.

25 Suhara Y, Watanabe M, Motoyoshi S, et al. Synthesis of new vitamin K analogues as steroid and xenobiotic receptor (SXR) agonists: insights into the biological role of the side chain part of vitamin K. Journal of Medicinal Chemistry. 2011; 54:4918-22.

26 Hirose T, Horvitz HR. An Sp1 transcription factor coordinates caspase-dependent and -independent apoptotic pathways. Nature. 2013; 500:354–358.

ACCEPTED MANUSCRIPT

27 Mohammad RM, Muqbil I, Lowe L, et al. Broad targeting of resistance to apoptosis in cancer. Seminars in Cancer Biology. 2015; 35:S78–S103.

28 Raza H, John A, Benedict S. Acetylsalicylic acid-induced oxidative stress, cell cycle arrest, apoptosis and mitochondrial dysfunction in human hepatoma HepG2 cells. European Journal of Pharmacology. 2011; 668:15-24.

29 Gara RK, Srivastava VK, Duggal S, et al. Shikonin selectively induces apoptosis in human prostate cancer cells through the endoplasmic reticulum stress and mitochondrial apoptotic pathway. Journal of Biomedical Science. 2015; 22:26.

30 Ji YB, Qu ZY, Zou X. Juglone-induced apoptosis in human gastric cancer SGC-7901 cells via the mitochondrial pathway. Experimental and Toxicologic Pathology : Official Journal of the Gesellschaft Fur Toxikologische Pathologie. 2011; 63:69-78.

31 Kee JY, Han YH, Kim DS, et al. β-Lapachone suppresses the lung metastasis of melanoma via the MAPK signaling pathway. PLoS ONE. 2017; 12:e0176937.

32 Wu X, Wang Y, Wang H, Wang Q, Wang L, Miao J, Cui F, Wang J. Quinacrine inhibits cell growth and induces apoptosis in human gastric cancer cell line SGC-7901.Curr Ther Res Clin Exp. 2012; 73:52–64.

33 Malumbres M. Cyclin-dependent kinases. Genome Biol. 2014; 15:122

34 Bendris N, Lemmers B, Blanchard JM. Cell cycle, cytoskeleton dynamics and beyond: the many functions of cyclins and CDK inhibitors. Cell Cycle. 2015; 14:1786–98.

35 Dickinson BC, Chang CJ. Chemistry and biology of reactive oxygen species in signaling or stress responses. Nature Chemical Biology. 2011; 7:504–511.

36 Holmström KM, Finkel T. Cellular mechanisms and physiological consequences of redox-dependent signalling. Nature Reviews. Molecular Cell Biology. 2014; 15:411-21.

37 Valavanidis A, Vlachogianni T, Fiotakis K, Loridas S. Pulmonary Oxidative Stress, Inflammation and Cancer: Respirable Particulate Matter, Fibrous Dusts and Ozone as Major

ACCEPTED MANUSCRIPT

Causes of Lung Carcinogenesis through Reactive Oxygen Species Mechanisms. International Journal of Environmental Research and Public Health. 2013; 10:3886–3907.

38 Xu C, Wang X, Zhu Y, et al. Rapamycin ameliorates cadmium-induced activation of MAPK pathway and neuronal apoptosis by preventing mitochondrial ROS inactivation of PP2A. Neuropharmacology. 2016; 105:270–284.

39 Gupta SC, Hevia D, Patchva S, et al. Upsides and Downsides of Reactive Oxygen Species for Cancer: The Roles of Reactive Oxygen Species in Tumorigenesis, Prevention, and Therapy. Antioxidants & Redox Signaling. 2012; 16:1295–1322.

40 Ray PD, Huang BW, Tsuji Y. Reactive oxygen species (ROS) homeostasis and redox regulation in cellular signaling. Cellular Signalling. 2012; 24:981–990.

41 Guo CL, Wang LJ, Zhao Y, et al. A Novel Bromophenol Derivative BOS-102 Induces Cell Cycle Arrest and Apoptosis in Human A549 Lung Cancer Cells via ROS-Mediated PI3K/Akt and the MAPK Signaling Pathway. Mar Drugs. 2018;16(2):43.

42 Zhan L, Cao H, Wang G, et al. Drp1-mediated mitochondrial fission promotes cell proliferation through crosstalk of p53 and NF-κB pathways in hepatocellular carcinoma. Oncotarget. 2016;7(40):65001-65011.

43 Oh B, Figtree G, Costa D, et al. Oxidative stress in prostate cancer patients: A systematic review of case control studies. Prostate Int. 2016; 4(3):71-87.

44 Ghosh SK, Ganta A, Spanjaard RA. Discovery and cellular stress pathway analysis of 1,4-naphthoquinone derivatives with novel, highly potent broad-spectrum anticancer activity. Journal of Biomedical Science. 2018; 25:12.

45 Qiu HY, Wang PF, Lin HY, et al. Naphthoquinones: A continuing source for discovery of therapeutic antineoplastic agents. Chemical Biology & Drug Design. 2017; 91:681–690.